

NO_x EMISSIONS FROM WOOD STOVES – A CFD MODELLING APPROACH

Mette Bugge^a, Nils E. L. Haugen^a, Øyvind Skreiberg^a
^aSINTEF Energy Research,
P.O. Box 4751 Sluppen, NO 7465 Trondheim, Norway

ABSTRACT: The present paper addresses NO_x emissions from wood stoves through a CFD modeling approach. In combustion of waste and biomass the most significant route for formation of NO_x is fuel NO_x. The formation of fuel NO_x is very complex and sensitive to fuel composition. Thus, accurate predictions of fuel NO_x formation in wood stoves, which constitute a wide range of compositions and states, rely heavily on the use of chemical kinetics with sufficient level of details. The computational fluid dynamics (CFD) simulations were performed using the *k-ε* turbulence model and the Eddy Dissipation Concept (EDC) by Magnussen [1][2] for turbulent combustion in conjunction with chemical reactions from a skeletal mechanism recently developed for biomass combustion [3]. The reaction mechanism includes 36 species. This work is a step in the development of a numerical tool required to study concept improvements with respect to NO_x emissions from wood stoves.

Keywords: Wood, combustion, NO_x emissions, CFD, reaction mechanism

1 INTRODUCTION

Today small-scale wood combustion in wood stoves accounts for half of the bioenergy use in Norway, and the use of wood logs in small-scale units and pellets in pellets stoves is expected to increase substantially towards 2020. The goal is to increase the energy conversion from these units by 8 TWh within 2020 [4]. That means that the energy conversion from these units has to be almost doubled compared with today. This calls for an increased effort with respect to emission reduction.

The present paper addresses NO_x emissions from wood stoves through a CFD modeling approach. There are very few papers on numerical simulations of wood log combustion available in the open literature. This is probably due to the complicated nature of such simulations, but also to the fact that the relevant industry historically has based its R&D purely on experiments. Of the few available papers on CFD of wood log combustion, a significant fraction has some connection with the Graz University of Technology.

In 2009 Scharler et al. [5] wrote a paper on CFD simulations of a commercial wood stove, where the simulations were used to optimize the stove by increasing the thermal efficiency at the same time as the emissions of CO and fine particulates were decreased. They used the realizable *k-ε* turbulence model and the eddy dissipation model with finite rate kinetics for the turbulence-combustion coupling. An extended version of a global 3-step methane mechanism was used for the gas phase chemical kinetics, while the discrete ordinates radiation model was used for the radiative heat transfer. A model developed for solid biomass combustion of fixed beds (space dependent) was modified to yield a time dependent volatile release model suitable for wood log combustion.

Scharler et al. (2011) [6] demonstrate how CFD can be used to develop, among other applications, wood stoves. They use an empirical sub-model designed for fixed bed combustion for the wood log combustion. A 3-step methane mechanism is coupled with EDM for the homogeneous chemistry. The simulations are stationary and post processing with EDC is used in order to obtain predictions for NO_x emissions. Ash production and deposition models are also used in the simulations.

Menghini et al. (2008) [7] performed experiments, simplified CFD simulations and theoretical analysis to investigate the importance of excess air on the efficiency

of a wood stove. It was found that the excess air ratio is a very important optimization parameter.

In addition to the above mentioned works there are a number of papers in the literature concerning CFD simulations of biomass combustion in small industrial furnaces (i.e. not in stoves for wood log combustion), e.g. Klason & Bai (2007) [8], Klason (2006) [9] and Shiehnejadhesar et al. (2013) [10].

2 THE MODELLING APPROACH

2.1 General

Computational Fluid Dynamics (CFD) is the analysis of systems involving fluid flow by means of computer-based simulations. These systems may also involve heat transfer and associated phenomena such as chemical reactions. CFD simulations are based upon a numerical solution of the basic equations of the fluid dynamics; conservation of mass, momentum, and energy, together with mathematical sub-models. The equations can be solved time-dependent and in three-dimensions. Comprehensive modelling of combustion in general requires simulation of turbulent fluid dynamics, chemical kinetics as well as their interactions.

The fundamental equations describing momentum, mass, energy and species evolution are well known and could in theory be solved in their most fundamental form. This is what in the literature is referred to as direct numerical simulations (DNS). Unfortunately, since this would require all spatial and temporal scales to be fully resolved, the number of grid points and time steps needed for simulations of domains of relevant size are far beyond what is available with today's computer clusters. For still some decades to come, one will therefore be forced to model the smallest scales of full scale applications using different kinds of modeling. This modelling is typically done by Reynolds averaging the Navier-Stokes equations (RANS), which corresponds to splitting an instantaneous quantity into its mean and fluctuating part.

In the current study, the ANSYS FLUENT software is used for the calculations. ANSYS FLUENT is the CFD software of choice for engineers and scientists in a wide area of disciplines. FLUENT 14 is a general-purpose CFD code, which is based on finite volumes. When using the finite volume method, the region of interest is divided

into small sub-regions called control volumes. The equations are discretized and solved iteratively, providing the value of each variable (velocity, temperature, mass fractions etc.) for each control volume throughout the calculation domain. A description of the CFD tool can be found on the ANSYS website (www.ansys.com), and a short description of the various models used is given in the section below.

2.2 Physical models

The equations for the RANS models used in ANSYS FLUENT are based on the fundamental form of the evolution equations, but in addition they also contain turbulence modeling terms. When assuming the fluid to be incompressible the set of RANS equations are given by: the continuity equation

$$\frac{\partial \bar{u}_i}{\partial x_i} = 0$$

the momentum equation

$$\frac{\partial}{\partial t}(\rho \bar{u}_i) + \frac{\partial}{\partial x_j}(\rho \bar{u}_i \bar{u}_j) = -\frac{\partial \bar{p}}{\partial x_i} + \frac{\partial}{\partial x_j}(\bar{\tau}_{ij} - \overline{\rho u'_i u'_j})$$

the energy equation

$$\frac{\partial}{\partial t}(\rho \bar{E}) + \frac{\partial}{\partial x_j}((\rho \bar{E} + p) \bar{u}_j) = \frac{\partial}{\partial x_j} \left(k_{eff} \frac{\partial T}{\partial x_j} - \sum_l h_l \bar{J}_l + (\bar{\tau}_{ij} - \overline{\rho u'_i u'_j}) \bar{u}_i \right)$$

and the species equation

$$\frac{\partial}{\partial t}(\rho \bar{Y}_k) + \frac{\partial}{\partial x_j}(\rho \bar{Y}_k \bar{u}_j) = \frac{\partial}{\partial x_j} \left(\rho D \frac{\partial \bar{Y}_k}{\partial x_j} - \overline{\rho Y'_k u'_j} \right) + \bar{R}_k.$$

In the above u , ρ , p , T and E are velocity, mass density, pressure, temperature and energy, respectively. Furthermore Y_k is the mass fraction of species k , overbars means ensemble averaging, τ is the stress tensor, u'_i is the turbulent velocity fluctuation in direction i , k_{eff} is the effective (kinematic plus turbulent) thermal conductivity, h is the enthalpy and D is the species diffusion coefficient. The Reynolds stress terms, $\overline{\rho u'_i u'_j}$, are found from the turbulence model, which in this work is the realized Reynolds number k - ϵ model with log-law wall functions. This model requires two partial differential equations to be solved; one equation for the turbulence energy, k , and one for the turbulence energy dissipation rate.

The interaction between turbulence and combustion is modelled with the Eddy Dissipation Concept (EDC) [1][2], and it yields the source term for species k ; \bar{R}_k . EDC is a reactor concept which identifies a reactor related to the fine structures in turbulence. This reactor is treated as a homogeneous reactor, exchanging mass and energy with the surrounding fluid, thus allowing a complete treatment of the chemistry of the reactor. The mass fraction of fluid within the fine structures, and the mass exchange rate between the fine structures and the

surrounding fluid, can be calculated on the basis of the turbulence.

For comparison, the laminar assumption has been made in a few of the simulations performed here. This means that no turbulence models are used, i.e. that the EDC model is substituted with plain Arrhenius reactions, that the effective conductivity is equal to the molecular conductivity and that the turbulence terms in the fluid equations: $\overline{\rho u'_i u'_j}$ and $\overline{\rho Y'_k u'_j}$, are zero.

The chemical kinetic mechanism used in the present work includes 214 elementary reactions among 36 species (Løvås et al. 2013[3]). It consists of reaction sets for hydrogen, C1-C2 hydrocarbons, HCN and NH₃ together with a subset of reactions describing the interaction between hydrocarbons and nitrogen species. It is a skeletal mechanism reduced down from a detailed chemical mechanism containing 1401 reactions and 81 species. The original detailed mechanism consists of several sub-models for important reaction paths known in biomass combustion. The reaction mechanism is developed for the prediction of NO_x formation in biomass combustion.

Whenever significant temperature differences are present within a given domain, radiative heat transfer may be of importance. In this work a discrete ordinates method (DO) is used to model the radiative transfer. In the DO method the radiative transfer equation (RTE), which has been transformed into a (non-transient) transport equation, is solved along a given set of directions. For each octant the radiation is discretized in two rays for both angular directions, meaning that the DO is solved along a total of 32 directions for the full hemisphere.

A soot model is used in order to account for the effect of soot formation, which for the current setup primarily is important for its contribution to the radiative cooling of the gas. The soot model chosen is the Moss & Brookes model, which solves transport equations for normalized radical nuclei concentration and soot mass fraction. The soot precursor is acetylene and ethylene (C₂H₂ and C₂H₄), which means that the nucleation rate is proportional to the concentration of acetylene, while the dominating soot oxidizing agent is OH.

2.3 Geometry model and boundary conditions

The wood stove chosen is a 5 kW natural draught wood log stove. The total combustion chamber volume is 0.0266m³, and the wood amount is 2kg based on the Norwegian standard NS 3058/3059. Primary air is injected through slots at the bottom of the stove, secondary air through 13 holes from the backside of the stove and flushing air is injected vertically through a slot above the front glass window.

The model is 3-dimensional and in full scale. As the stove is symmetrical, a symmetry boundary is defined through the vertical center plane, which means that the model includes one half of the stove (Figure 1). The geometry has been gridded with the ANSYS meshing platform (AMP). The mesh consists of approximately 256 000 tetrahedral elements.

The wood logs are represented as volumes. The thermochemical conversion of the solid fuel is not included in the CFD-calculations. The volatiles are released from the outer surfaces of the wood pile.

Wood-log combustion is a batch process including drying, pyrolysis, gasification, combustion of carbon as

well as combustion of the gas components. The release of volatiles from the wood log is time dependent with respect to mass flow and gas composition. A model for the gas release has been developed.

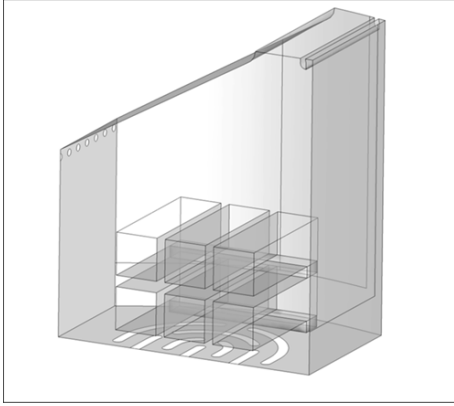


Figure 1: The wood stove model

The gas composition and flow is based on Norway spruce, a wood consumption of 1.5 kg/h and the specific excess air ratio ($\lambda_p = 0.8$). The gas composition has been optimized towards satisfying available relevant pyrolysis gas compositions and char gasification while maintaining the elemental balances for the solid fuel.

Table I shows the composition of the fuel gas/primary air mixture based on a primary excess air ratio of 0.8. The amount of primary air injected through the slots corresponds to the excess oxygen in this composition. Increasing the primary excess air ratio will only change the mass of oxygen (O_2) and nitrogen (N_2), diluting the fuel gas. The mass of the combustible components will remain unchanged while the mass flow

Table I: Composition of fuel gas/primary air mixture for primary excess air ratio (λ_p) of 0.8

Specie	wt%	g
CO ₂	4.1016	286.2761
H ₂ O	7.0759	493.8693
CO	12.5715	877.4385
H ₂	0.2609	18.2101
CH ₄	1.3293	92.7789
C ₂ H ₂	0.0539	3.7646
C ₂ H ₄	0.5811	40.5602
C ₂ H ₆	0.3114	21.7374
NO	0.0011	0.0735
HCN	0.0075	0.5215
NH ₃	0.0072	0.5055
O ₂	13.3430	931.2863
N ₂	59.3434	4141.9418
Ar	1.0122	70.6486
Tot gas	100.0000	6979.6123
Ash		4.9200
Total		6984.5323

of primary air injected through the bottom slots will increase. The gas temperature is set to 773K.

The mass flow of volatiles released from the wood logs is determined by the heat flux from the combustion zone which means that the surfaces that are most visible to the flames will have the highest release. In this work the relative ratio between the release velocity for the top, side and end surfaces of the wood pile are 1/0.25/0.375.

The stove has cast iron walls, an insulated combustion chamber and a front glass window. In this work all the walls are treated identical, as isothermal walls with temperature 673K, and hence the radiation heat loss through the front glass window is neglected. In this initial work this is regarded as justifiable assumptions.

In the base case, the total excess air ratio is 1.6, the fraction of primary/secondary/flushing air is 0.5/0.4/0.1, and the air temperatures used are 300, 373 and 623K, respectively. Several air distributions and excess air ratios are studied, as well as the effect on the NOx emission level.

3 RESULTS AND DISCUSSION

3.1 Base case

The fuel gas is released from the outer surfaces of the wood pile. The major part is released from the top surface, and the fuel conversion occurs mainly above the wood pile where the secondary air is injected, but also to an extent where the fuel gas from the side and end faces meets the primary air. As shown in Figure 2 the simulations give elevated temperatures in these areas. The maximum temperature is 1600K. The mean outlet temperature obtained in the simulations is 910 K.

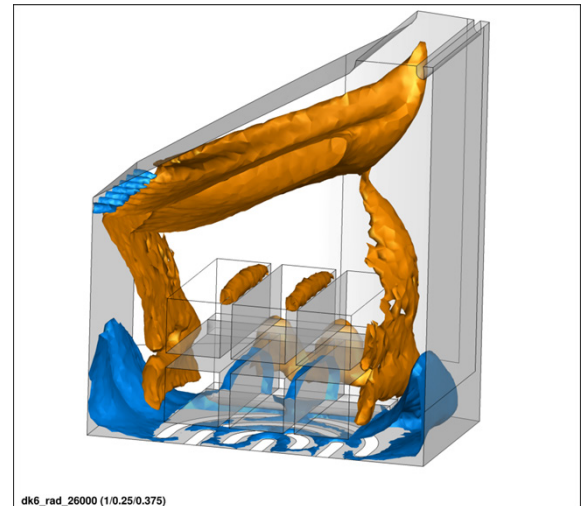


Figure 2: Iso-surfaces for temperatures of 600 and 1100K for base case

Figure 3 shows the mass flow rate of carbon in CO and CH₄ along the stove height. It can be seen that CO increases slightly from the bottom of the stove to about 0.12m followed by a steep increase up to 0.14m. This profile corresponds well with the fuel gas release with a low release from the side and end faces and a higher release from the top face. There is also a contribution due to the production of CO from hydrocarbon fuel gas components. In the upper part of the stove, where sufficient air is available, there is a net reduction of CO.

The CH₄ profile is similar to the CO profile however some CH₄ reacts in the lower part in contrast to CO which is formed, partly from CH₄.

The NH₃ and HCN profiles shown in Figure 3 correspond well with the fuel gas release in the lower part of the stove, and the mass flow rates of these components are reduced along the stove height. NO is formed when NH₃ and HCN are reduced, while there is a certain reduction of this NO in the upper part of the stove when the secondary air is injected. NO₂ is increasing in the upper part of the stove. HCN is reduced to a much lesser extent than NH₃ in the upper part of the stove, indicating that HCN is partly formed from NH₃. A reaction path analysis would be needed to follow the nitrogen flow through the fuel NO_x mechanism.

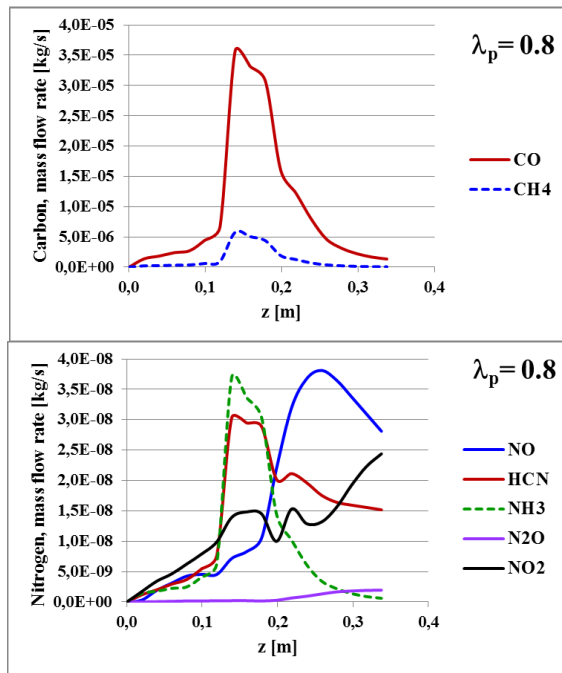


Figure 3: Mass flow rates [kg/s] along the wood stove height. Upper: Carbon in CO and CH₄. Lower: Nitrogen in selected species

Removing the nitrogen components (NO, HCN and NH₃) from the fuel gas, prevents the formation of fuel NO_x and allows to check the contribution from the other NO_x formation mechanisms to the NO_x emission level. As the temperatures are below 1700K, the production of thermal NO_x is negligible. However, the simulations still predict NO_x formation, which indicates formation of prompt NO_x. As the reduced mechanism do not contain the traditional prompt NO_x initiating reactions (they were automatically removed in the necessity analysis in the mechanism reduction process), there must be other initiating reactions converting molecular nitrogen to a nitrogen species that can be further converted to NO. The simulations actually predict that approximately 50% of the NO_x is prompt NO_x, and the fraction is almost the same when comparing TFN (total fixed nitrogen) including NO₂, N₂O, HCN and NH₃ in addition to NO. This prompt NO_x fraction is considerable higher than expected. Corresponding CFD simulations comparing the 36 species mechanism used in the present work with the full detailed mechanism (81 species) indicates that the skeletal mechanism overestimates the prompt NO_x formation 20 times and the NO₂ formation 5 times. Løvås

et al. [3] found that the gas concentrations predicted with the 36 species mechanism was in agreement with the master mechanism at higher temperatures (1073K), but the NO_x concentrations could be overestimated at lower temperatures (873K). In the present CFD study the temperatures are lower than 1073K in a significant part of the domain (Figure 2).

3.2 The effect of air distribution

The effect of air injection and distribution are studied through several scenarios as shown in Table II. The total excess air ratio is 1.6 in all scenarios, and the ratio between flushing and secondary air is kept constant (1/4). The predicted effect of prompt NO_x is investigated for the staged air cases by running simulations both with and without fuel nitrogen.

Table II: Simulation scenarios

Case	Primary excess air ratio, λ_p	Fuel-N
Base (LP08)	0.8	Y
LP09	0.9	Y
LP095	0.95	Y
LP1_6	1.6	Y
LP08_Pno	0.8	N
LP09_Pno	0.9	N
LP095_Pno	0.95	N

According to the simulations, the NO emissions are nearly the same for all the scenarios (Figure 4). The prompt NO formation is decreasing when the primary excess air ratio is increasing, giving leaner conditions. However, the relative prompt NO contribution is higher than expected for all the scenarios.

Previous studies [11][12] have shown that air staging could be an efficient method to reduce NO_x emissions. Even if the present wood stove is not a classic air staged scenario as the mixing of fuel gas and primary air is far from complete before the secondary air is injected, some effect could be expected.

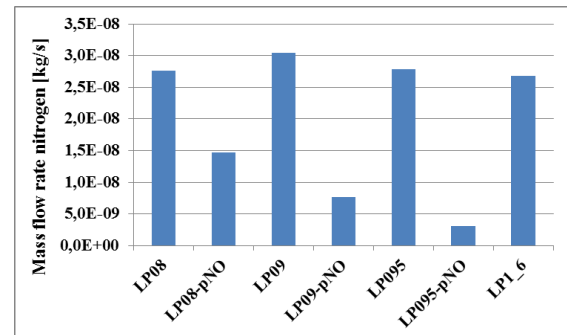


Figure 4: The simulation results of NO emission at the outlet, mass flow rate of the nitrogen fraction of NO [kg/s]

As shown in Figure 3 the simulations predict significant values of NO₂ and also HCN at the outlet, and hence it could be useful to compare the values of total fixed nitrogen (TFN) including NO₂, N₂O, HCN and NH₃

in addition to NO (Figure 5). It can be seen that there is a slight increase in the TFN with increasing primary excess air ratio. For the scenarios without nitrogen in the fuel gas, the TFN is decreasing with increasing primary excess air ratio.

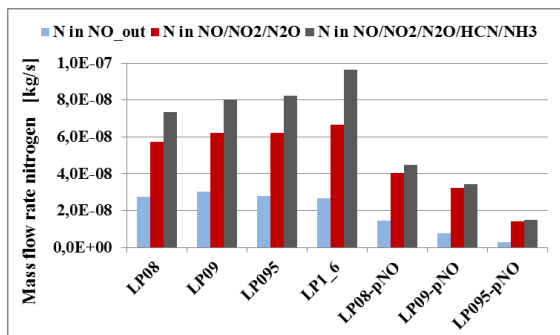


Figure 5: The simulation results of TFN emission at the outlet, mass flow rate of the nitrogen fraction of the TFN components [kg/s]

Figure 6 shows the NO emissions taking into account that the simulations over predict the prompt NO contribution by assuming that the real contribution is 5% of the simulated value for all the staged air scenarios. Primary excess air ratios of 0.9 and 0.95 give a slight reduction in NO compared to no air staging, while 0.8 give a significant reduction (50%).

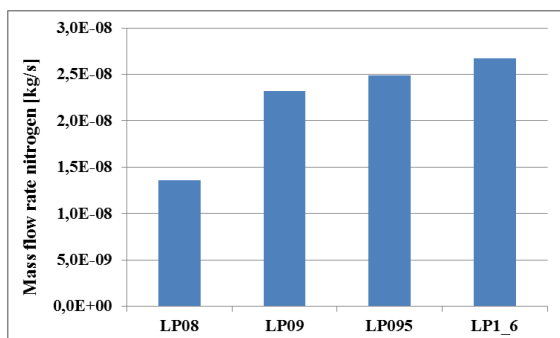


Figure 6: The NO emission at the outlet with corrected prompt NO_x contribution for the staged air cases, mass flow rate of the nitrogen fraction of NO [kg/s]

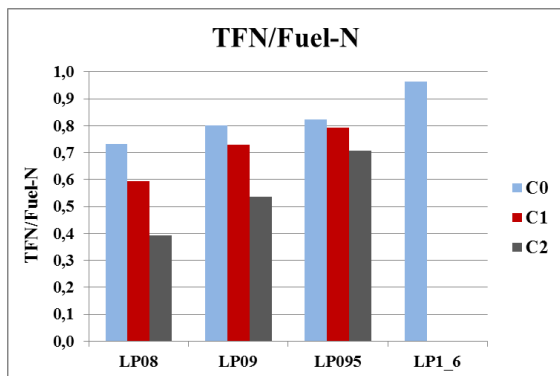


Figure 7: TFN/Fuel-N ratio at the outlet. C0-simulation results, C1 – prompt NO correction included, C2 – correction included for prompt NO and NO₂

The TFN/Fuel-N ratio is compared in Figure 7. The C0 case represents the simulation results and show a

slight increase with increasing primary excess air ratio, as described previously (Figure 5). The correction 1 (C1) case assumes that the real prompt NO contribution is 5% of the simulated value for all the staged air scenarios, while the correction 2 (C2) case has the additional assumption that the real NO₂ from the prompt mechanism is 20% of the simulation result for all the staged air cases.

It can be seen that for a primary excess ratio of 0.8 the C1 and C2 assumptions give a TFN/Fuel-N ratio of 0.6 and 0.4 respectively, which represent a significant reduction. The ratio is increasing with increasing λ_p for both assumptions.

Summarizing, the simulations give a significant NO_x reduction at a primary excess air ratio of 0.8, showing the potential of NO_x reduction by staged air combustion. However, a further reduction may be achieved at an even lower primary excess air ratio. The simulations also demonstrate one of the main challenges with CFD modelling of wood stoves, the reliability of the chemical kinetics applied over the complete range of conditions within the combustion chamber, from very fuel-rich to very fuel-lean conditions and over a large temperature span.

In our case a significant part of the nitrogen chemistry has taken part in a relatively low temperature range where the skeleton mechanism applied has the weakness of over predicting the NO formation. In our case this over prediction has been corrected for using knowledge from corresponding CFD simulations using the full mechanism. In future work a less reduced skeleton mechanism should be implemented to avoid the over prediction, which in practice should result in reduced net conversion of nitrogen from the air through untraditional prompt NO_x initiating reactions. Alternatively, a reaction path analysis may reveal one or a few critical initiating reactions, where the rate constant could be tuned to match results from the full mechanism. However, this last approach is a non-physical approach, and maintaining the rate constants of the elementary reactions in the full mechanism in the skeleton mechanism should be the goal.

4 CONCLUSIONS

As a step in the development of a numerical tool to study concept improvements with respect to NO_x emissions from wood stoves, a CFD based model for wood log fired stoves is developed. The model includes chemical reactions from a recently published 36 species skeletal mechanism for biomass combustion [3].

The simulations show that the skeletal mechanism over predicts the prompt NO_x formation at the conditions in this study, relatively low temperatures in a significant part of the domain. In the present work this over prediction has been corrected for using knowledge from corresponding CFD simulations using the full mechanism. The results give a significant NO_x reduction at a primary excess air ratio of 0.8, showing the potential of NO_x reduction by staged air combustion.

Future work will include simulations with a less reduced skeletal mechanism. Improvement of the skeletal mechanism used in the present work could also be considered.

5 REFERENCES

- [1] I. Gran and B.F. Magnussen, Comb. Sci. Technol. 119, 1996
- [2] I. Ertesvåg and B.F. Magnussen, Comb. Sci. Technol. 159, 2000
- [3] T. Løvås, E. Houshfar, M. Bugge, Ø. Skreiberg, Energy & fuels, 2013, 27(11), 6979-6991
- [4] Regjeringen. Strategi for økt utbygging av bioenergi. 2008; Available from:
<http://www.regjeringen.no/nb/dep/oed/dok/rapporter/2008/strategi-for-okt-utbygging-av-bioenergi.html?id=505401>
- [5] R.Scharler, C. Benesch, A. Neudeck, I. Obernberger, Proceedings of the 17th European Biomass Conference and Exhibition, 2009; pag. 1361-1367
- [6] R. Scharler, C. Benesch, K. Schulze, I. Obernberger, Proceedings of the 19th European biomass conference and exhibition, June 2011, Berlin, Germany
- [7] D. Menghini, F.S. Marra, C. Allouis, F. Beretta, Experimental Thermal and Fluid Science 32 (2008), 1371–1380
- [8] T. Klason, X.S. Bai, Fuel 86 (2007) 1465–1474
- [9] T. Klason, Doctoral thesis, Lund Institute of Technology, 2006, ISBN 91-631-8870-8
- [10] A. Shiehnejadhesar, K. Schulze, R. Scharler, I. Obernberger, Biomass and bioenergy 53 (2013) 48-53
- [11] E. Houshfar, Ø. Skreiberg, T. Løvås, D. Todorovic, L. Sørum, Energy & Fuels, 2011, 25, 4643-4654
- [12] Ø. Skreiberg, J.E. Hustad, E. Karlsvik. In Developments in Thermochemical Biomass Conversion, Banff, Canada, 1996, A.V Bridgewater, D.G.B. Boocock, Eds. Blackie Academic & professional: London, UK, 1997, pp 1462-1478

6 ACKNOWLEDGEMENTS

The authors acknowledge the financial support from the Research Council of Norway and the four industrial partners in the StableWood project. The industrial partners in the StableWood project are:

